Neural–Cardiac Coupling in Threat-Evoked Anxiety

Kim M. Dalton, Ned H. Kalin, Thomas M. Grist, and Richard J. Davidson

Abstract

■ Anxiety is a debilitating symptom of many psychiatric disorders including generalized anxiety disorder, mood disorders, schizophrenia, and autism. Anxiety involves changes in both central and peripheral biology, yet extant functional imaging studies have focused exclusively on the brain. Here we show, using functional brain and cardiac imaging in sequential brain and cardiac magnetic resonance imaging (MRI) sessions in response to cues that predict either threat (a possible shock) or safety (no possibility of shock), that MR signal change in the amygdala and the prefrontal and insula cortices predicts cardiac contractility to the threat of shock. Participants with greater MR signal change in these regions show increased cardiac contractility to the threat versus safety condition, a measure of the sympathetic nervous system contribution to the myocardium. These findings demonstrate robust neural–cardiac coupling during induced anxiety and indicate that individuals with greater activation in brain regions identified with aversive emotion show larger magnitude cardiac contractility increases to threat. ■

INTRODUCTION

Research on the neurobiology of anxiety has focused mainly on the central and endocrine components of this affective state. However, empirical and theoretical research clearly indicates that both central and peripheral biological changes are fundamental to a complete account of anxiety (Davidson, 2002). Whereas neuroimaging methods have helped to establish the important roles of the prefrontal cortex (PFC) (Rauch, Savage, Alpert, Fischman, & Jenike, 1997), amygdala (Davis & Whalen, 2001), and insula (Critchley, Corfield, Chandler, Mathias, & Dolan, 2000) in anxiety, preciously little, other than surface autonomic measures, have been used to characterize the peripheral changes that accompany anxiety. More precise measures are required to disentangle the sympathetic and parasympathetic contributions to most surface-recorded autonomic measures (Brownley, Hurwitz, & Schneiderman, 2000). This is particularly true for cardiovascular measures because the myocardium is innervated by sympathetic and parasympathetic efferents.

Cardiac contractility arises primarily from the sympathetic innervation to the myocardium. It is only during extreme tachycardia when parasympathetic input significantly affects cardiac contractility (Brownley et al., 2000). However, relatively few studies report a true index of cardiac contractility because it requires direct measurement of the myocardium in motion. Recent advances in magnetic resonance imaging (MRI) myocardial tagging techniques with concurrent breath-hold allow for such measures by rapidly acquiring cross-sectional images through the left ventricle at several points during the cardiac cycle. These images can then be used to calculate thickening of the myocardium (or contraction of the ventricular cavity) from maximum diastole (relaxation) to maximum systole (contraction), providing a relatively pure index of cardiac contractility and sympathetic tone.

Increases in cardiac contractility likely play a key role in the somatic distress of anxiety (Brownley et al., 2000). Moreover, modern pharmacological treatments of anxiety include beta-blockers that attenuate the sympathetic autonomic changes that occur during this state, thus decreasing the direct somatic symptoms of anxiety and also attenuating peripheral feedback to central targets that serve to further activate the central circuitry of anxiety (Grippo, Moffitt, & Johnson, 2002). Finally, studies using electrical stimulation and lesion methods in animals have confirmed that the amygdala, insula, and PFC all play a key role in regulating cardiovascular responses and in the monitoring of peripheral cardiovascular reactivity (Spyer, 1994).

The role of the amygdala in aspects of emotional processing has been extensively documented (for a review, see Zald, 2003). A vast amount of that research has focused on the role of the amygdala in conscious and unconscious processing of fear (Morris, Ohman, & Dolan, 1999; Buchel, Morris, Dolan, & Friston, 1998; LaBar, Gatenby, Gore, LeDoux, & Phelps, 1998) and conditioned and learned fear (Phelps et al., 2001). Furthermore, the amygdala has been implicated in autonomic arousal in response to fear (Critchley, Mathias, & Dolan, 2002). The amygdala also has extensive and

University of Wisconsin

reciprocal connections with other areas involved in autonomic arousal and regulation such as the insula (Shi & Davis, 1999).

A large body of research suggests a role of the insula cortex in cardiac regulation, with some evidence that the right insula in particular may play a role in mediating sympathetic myocardial activity (Critchley, Corfield, et al., 2000; Wittling, Block, Schweiger, & Genzel, 1998). In fact, the insula cortex has been proposed as a crucial mediator of stress-induced cardiovascular responses in a rat stroke model (Cechetto, 1994). Evidence for the role of the insula cortex in stress-induced cardiovascular responses also comes from the role of the insula cortex in conveying sensory information to the orbitofrontal cortex (OFC) and amygdala (Augustine, 1996).

We sought to study the coupling between neural and cardiac changes in anxiety by using functional brain and cardiac MRI in the same subjects, in sequential MRI sessions, in response to the same task designed to experimentally induce anxiety. Most importantly, this design enabled us to directly examine relations between neural and cardiac changes induced by threat.

We tested the hypothesis that acute anxiety is associated with activation in the amygdalae, PFC, and insula cortices and that activation in these regions may be involved in the regulation of sympathetic input to the myocardium and therefore play a role in mediating stress-related cardiac reactivity. We acquired functional brain and cardiac images using an event-related paradigm during a modified instructed fear task as well as during a control safety period (Phelps et al., 2001).

RESULTS

Heart Rate

Seventeen of the 23 participants displayed a clear bradycardia to the threat versus safe trials during the brain scan as evidenced by an average decrease of at least 1 bpm from baseline and a consistent inverse quadratic shape in heart rate (HR) over the course of the threat trials (see Figure 1). These 17 participants had a significantly lower HR to the threat versus safe condition during the brain scan, $t(1,16) = 6.91$, $p < .0009$. Eight of the 17 selected subjects had the brain scan first; the remaining 9 had the cardiac scan first. There was no significant difference in average HR between the safe and threat trials during the cardiac scan due to the breath-hold-induced bradycardia during both the safe and threat trials. All further analyses were restricted to those 17 participants who displayed a clear bradycardia to the threat trials in order to directly assess activations in cortical and subcortical regions associated with a consistent pattern of stress-induced cardiac reactivity. Only HR recorded during the brain scan is included in further analyses due to the confounding breath-hold-induced bradycardia during the cardiac scan.

Self-reported Anxiety and Pain

The 17 selected subjects reported a moderate level of anxiety in response to the threat of shock condition ($M = 8.66$, $SD = 4.86$) and rated the actual shocks as moderately painful ($M = 6.97$, $SD = 4.04$) across both the

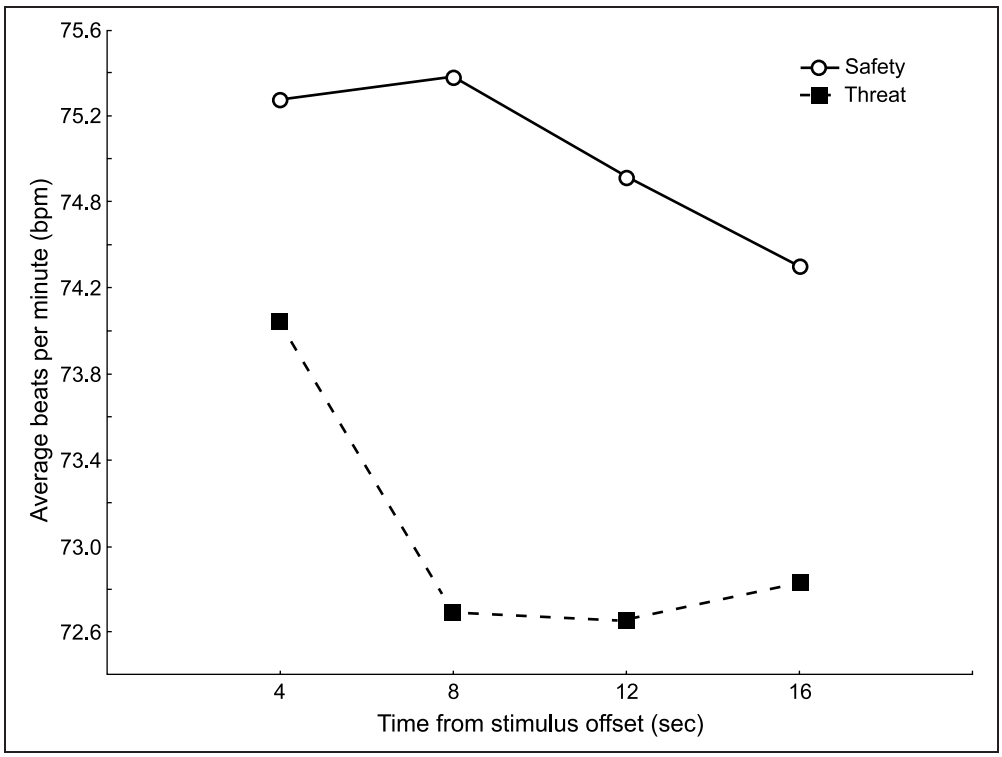

Figure 1. Average HR across the safe ($M = 74.9$, $SD = .44$) and threat trials ($M = 73.3$, $SD = .57$) for the 17 participants who displayed a clear and significant bradycardia to the threat trials as defined as a minimum of 1 bpm decrease and a consistent inverse quadratic trend across the threat trials.

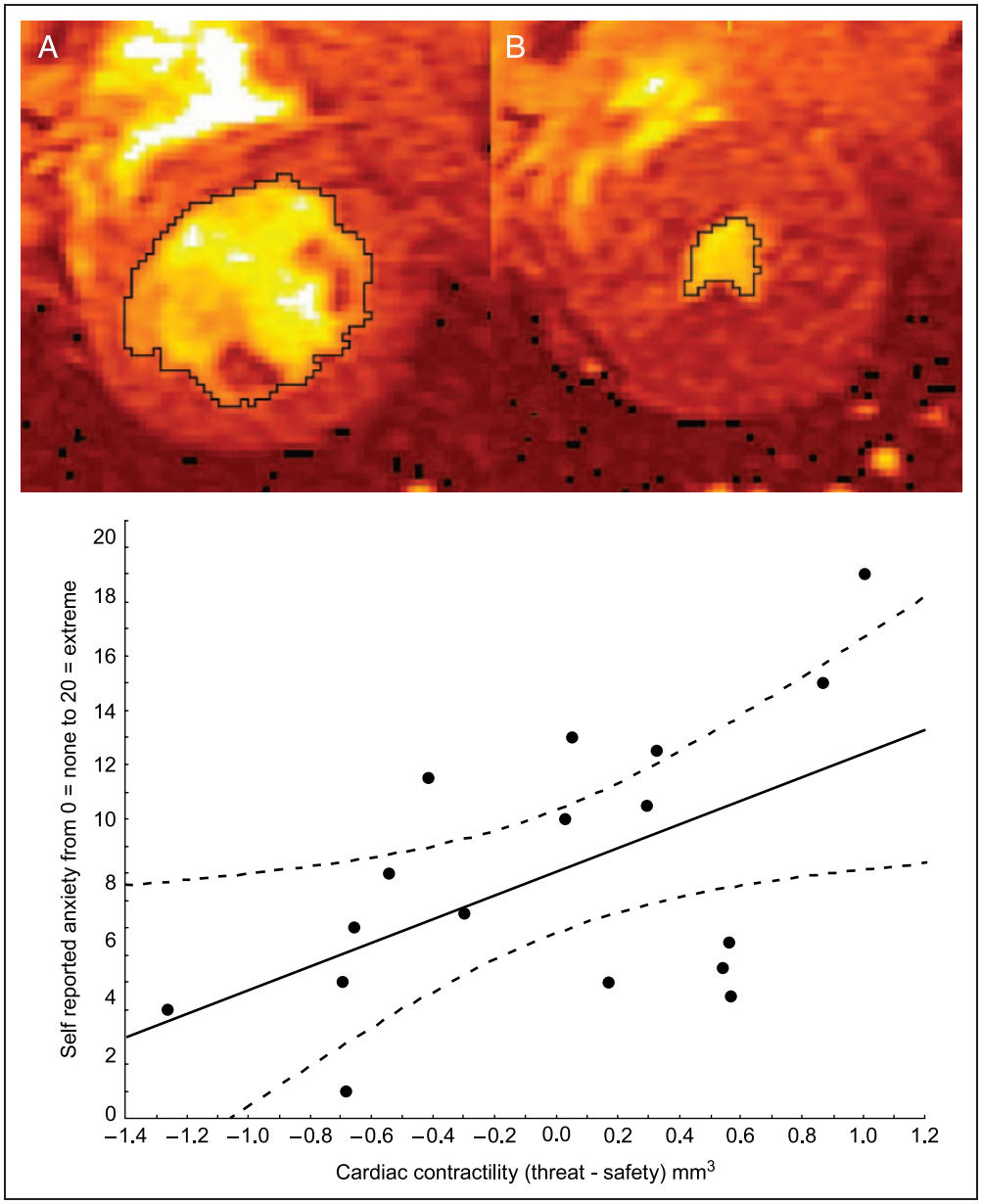

Figure 2. Top: MRI cross-sectional images of the left-ventricle at (A) maximum diastole, full relaxation, and (B) maximum systole, full contraction. The area of the left ventricle (in cubic millimeters) was extracted using an automated edge detector function of SPAM (Oakes, University of Wisconsin, Madison, WI). Each area was then manually inspected and edited as needed. The difference in area of the left ventricle (outlined in black) between maximum relaxation and maximum contraction was calculated as an index of myocardial contractility. Bottom: Scatter plot of significant correlation between self-report anxiety and cardiac contractility during threat versus safety ($r = .548$, $p = .023$).

brain and cardiac scans. There was no significant difference between anxiety reported during the brain scan ($M = 9.03$, $SD = 5.02$) and anxiety reported during the cardiac scan, $M = 8.29$, $SD = 5.33$, $t(1,16) = 0.84$, $p = .41$. Similarly, the average pain intensity was statistically equivalent for both the brain ($M = 7.05$, $SD = 3.99$) and cardiac ($M = 6.88$, $SD = 4.20$) scans, $t(1,16) = 0.45$, $p = .66$. There were no significant differences in either reported anxiety or pain between the first and second scans (i.e., no order effect or significant habituation for experienced anxiety or pain). Pain ratings were not significantly correlated with general anxiety, state anxiety, or anxiety to the threat of shock during either the brain or cardiac scan. Trait anxiety was not significantly correlated with either state anxiety during the session or self-reported anxiety during either the brain or cardiac scan. Similarly, state anxiety was not significantly correlated with self-reported anxiety during either the brain or cardiac scan. Both self-reported anxiety to the threat of shock and pain ratings were negatively correlated with change in HR (threat minus safety) during the brain scan ($r = -.61$, $p = .01$; $r = -.53$, $p = .03$, respectively); that is, the more anxiety provoking and painful the shock the larger the bradycardia to the threat versus safe condition.

Cardiac Contractility during Threat versus Safe Conditions

High-resolution cross-sectional images of the left ventricle were obtained at evenly paced intervals throughout the cardiac cycle during an 8–12 sec breath-hold segment of each trial following the anticipatory cue. Cardiac

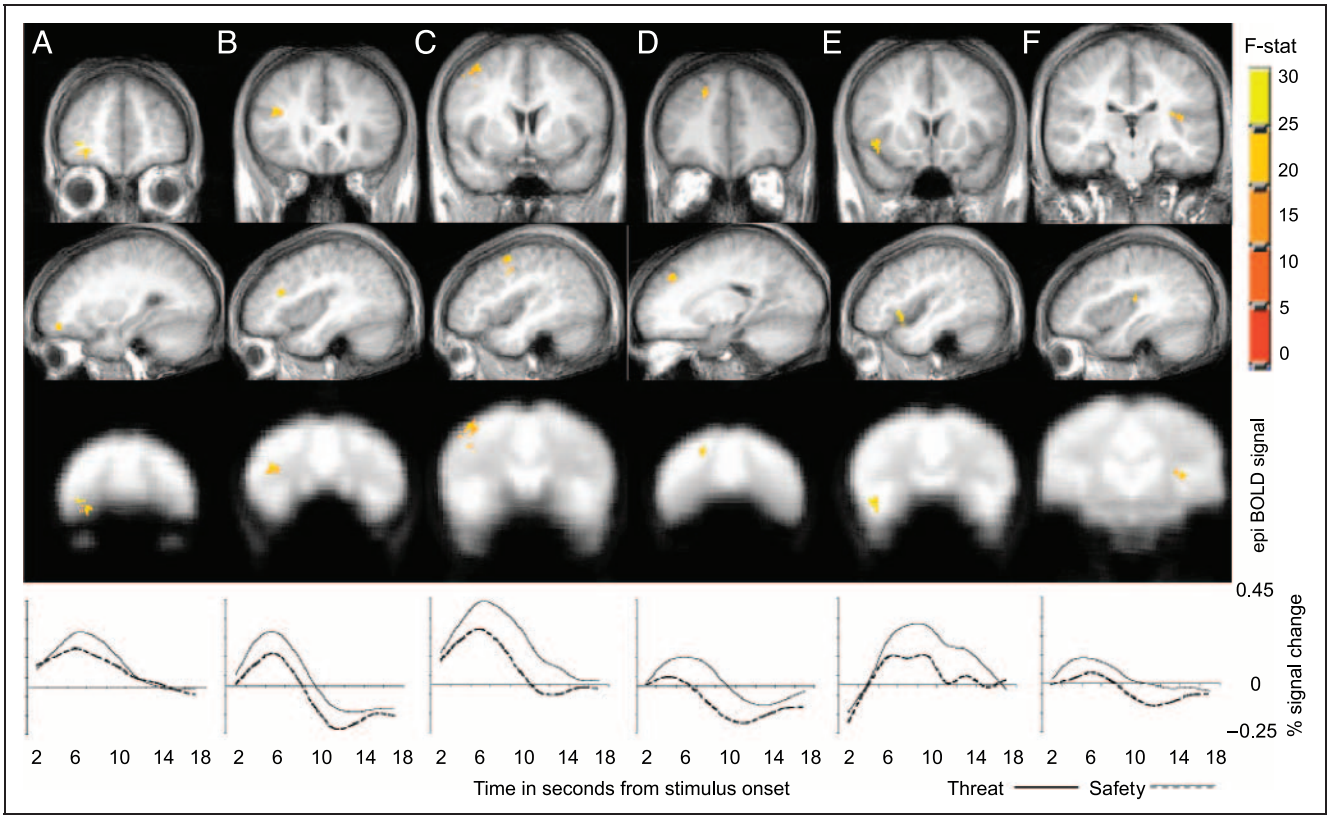

Figure 3. Brain regions associated with greater activation to the threat versus safety condition. The first two rows display the location and size of the clusters with the color of the cluster indexing the size of the effect. The third row is composed of the same clusters superimposed on an averaged EPI BOLD signal indicating good signal coverage for each cluster. The fourth row is the averaged hemodynamic response function for both the threat and safe conditions for each cluster. (A) Right orbitofrontal gyrus: $x = -28$, $y = 46$, $z = -12$; no. of voxels = 180; $F(1,16) = 19.53$, $p = .0004$. (B) Right inferior frontal gyrus: $x = -38$, $y = 24$, $z = 19$; no. of voxels = 177; $F(1,16) = 19.27$, $p = .0004$. (C) Right middle frontal gyrus: $x = -38$, $y = 5$, $z = 48$; no. of voxels = 520; $F(1,16) = 33.64$, $p = .00002$. (D) Right superior frontal gyrus: $x = -19$, $y = 36$, $z = 32$; no. of voxels = 140; $F(1,16) = 33.06$, $p = .00003$. (E) Right anterior insula, region Id: $x = -42$, $y = 12$, $z = -6$; no. of voxels = 178; $F(1,16) = 13.83$, $p = .002$. (F) Left posterior insula, region Ig: $x = 33$, $y = -19$, $z = 16$; no. of voxels = 146; $F(1,16) = 18.40$, $p = .0005$).

contractility was derived as the difference in area of the left ventricle slice from maximum diastole to maximum systole across each trial during the cardiac MRI scan (see Figure 2). No effect was found for threat versus safe conditions on cardiac contractility, $t(1,16) = .054$, $p = .95$. However, increases in cardiac contractility to the threat versus the safe conditions were significantly associated with self-reported anxiety to the threat condition, $r = .548$, $p = .023$ (see Figure 2). This indicates that greater anxiety to shock was associated with increased sympathetic activation during the threat versus safe conditions. Cardiac contractility was not correlated with

Table 1. Significant Valence × Hemisphere Interactions in Clusters of Activation during Threat versus Safety Condition

		Valence × Hemisphere Interaction		*Valence Simple Effects*			
				Right		*Left*	
	Blurred Cluster Size[a]	*F*	*p*	*F*	*p*	*F*	*p*
Lateral orbitofrontal gyrus	482	.39	.53	14.66	.001	1.59	.22
Anterior middle frontal gyrus	779	9.92	.006	30.07	.00005	2.06	.16
Posterior inferior frontal gyrus	406	32.94	.00003	13.25	.002	0.58	.46
Posterior superior frontal gyrus	303	7.89	.01	24.23	.0001	3.31	.08

[a]Cluster size is reported in cubic millimeters.

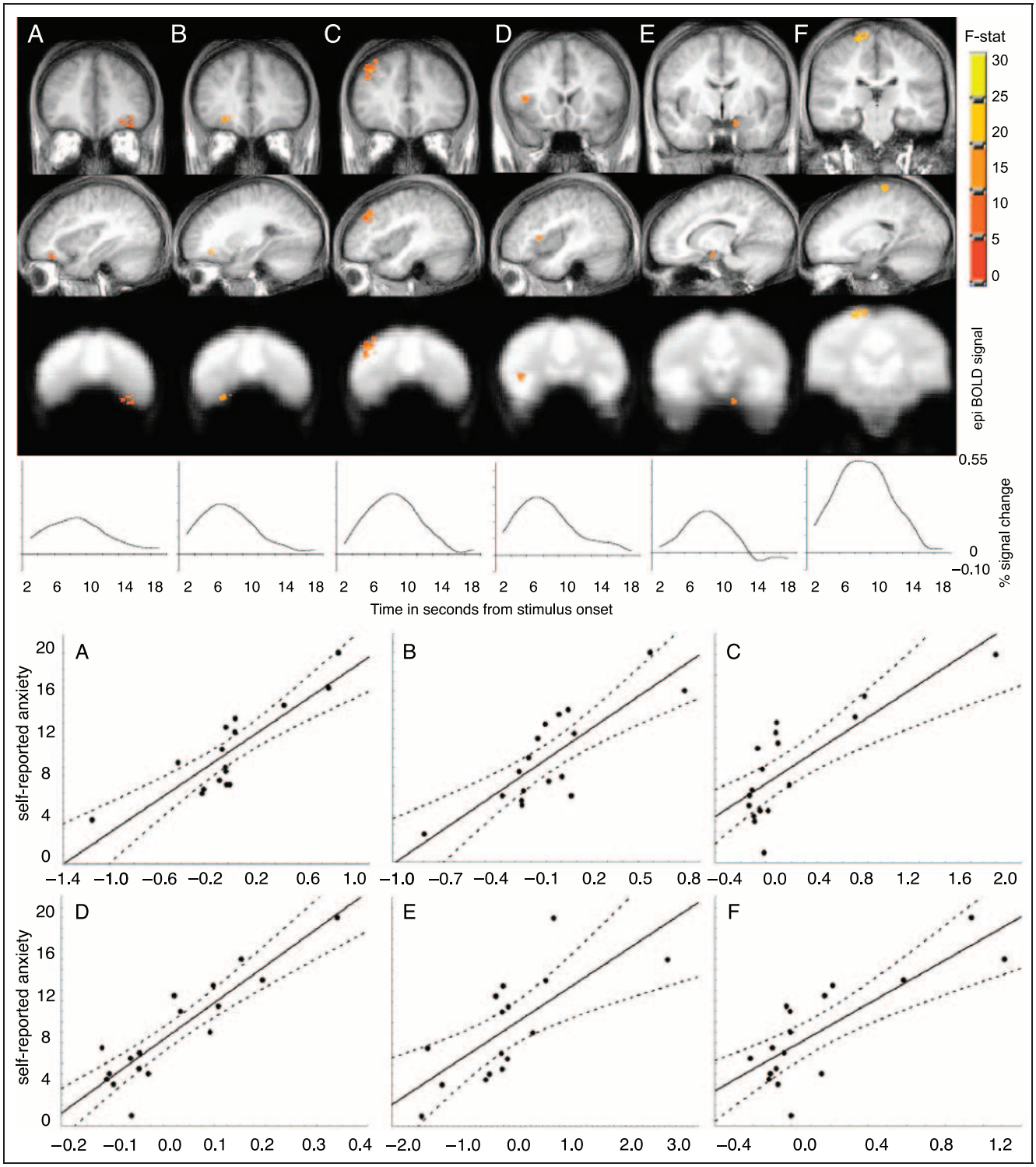

Figure 4. Clusters of brain activation (threat minus safety) positively associated with self-reported anxiety in anticipation of shock. The first two rows display the location and size of the clusters with the color of the cluster indexing the size of the effect. The third row is composed of the same clusters superimposed on an averaged EPI BOLD signal indicating adequate signal coverage for each cluster. The fourth row is the averaged hemodynamic response function to the threat condition for each cluster. The last two rows are the scatter plots for each cluster with self-reported anxiety on the x axis from 0 = no anxiety to 20 = extreme anxiety in anticipation to shock and percent signal change (threat minus safety) for each cluster on the y-axis. (A) Left orbitofrontal gyrus ($x = 27, y = 36, z = -16$; no. of voxels = 259; $r = .86$, $p < .0001$). (B) Right orbitofrontal gyrus ($x = -25, y = 31, z = -13$; no. of voxels = 284; $r = .81, p < .0001$). (C) Right middle frontal gyrus ($x = -37, y = 33, z = 33$; no. of voxels = 1126; $r = .78, p < .0001$). (D) Right anterior insula, region Ig ($x = -39, y = 13, z = 7$; no. of voxels = 285; $r = .90, p < .0001$). (E) Left dorsomedial amygdala ($x = 14, y = -5, z = -15$; no. of voxels = 67); $r = .71, p = .002$). (F) Right postcentral gyrus, sensory cortex ($x = -19, y = -25, z = 65$; no. of voxels = 509; $r = .79, p < .0001$).

either trait ($r = .06$, $p = .79$) or state ($r = .25$, $p = .33$) anxiety nor with self-reported pain associated with the shocks ($r = .24$, $p = .35$).

Brain Activation during Threat versus Safe Conditions

Increased activation to the threat versus safety condition was found in right-sided regions of the OFC, lateral PFC, and bilateral insula cortex (Figure 3). Activations were seen in three regions of the PFC, inferior, middle and superior frontal, and each of these activations was significantly greater in the right- compared with left-hemisphere homologous regions (see Table 1). Imaging parameters precluded examination of responses in the ventromedial PFC. There was no hemisphere effect for the lateral OFC cluster; however, the greater activation to the threat versus safe conditions was significant only in the right OFC.

Correlations between Brain Activation and Self-reported Anxiety

A regression was performed predicting brain activation to the threat versus safe condition using self-reported anxiety during the brain scan. Significant clusters of activation associated with self-reported anxiety were then extracted using a conservative threshold as described in the Methods section. Self-reported anxiety predicted brain activation to the threat versus safe condition in the bilateral OFC, right middle frontal gyrus, right anterior insula (region Ig), left amygdala, and right postcentral gyrus (see Figure 4).[1]

Correlations between Brain Activation and Cardiac Contractility

We next examined the relation between cardiac contractility and brain activation in response to the threat versus safe conditions by regressing cardiac contractility on brain activation to the threat versus safe trials using the same conservative threshold as described in the Methods section and above. Cardiac contractility predicted brain activation to the threat versus safe condition in clusters in the left medial amygdala, right posterior insula (region Id), and right middle frontal gyrus (see Figure 5). Participants with greater activation in these regions exhibited greater cardiac contractility to the threat versus safety conditions. Furthermore, those participants who showed an increase in cardiac contractility to the threat versus safe condition ($n = 10$) evidenced significantly greater activation in these regions than those participants ($n = 7$) who showed a decrease in contractility to the threat versus safe condition (see Figure 6). When activation in each of these clusters was entered into a regression to predict cardiac contractility, the multiple R^2 indicated that greater than 85% of the variance in cardiac contractility was predicted by the increase in activation in these clusters in response to the threat versus safety condition, $R^2 = .855$, $(3,13) = 25.54$, $p < .0001$.

The effects of possible interactions between cardiac contractility and self-reported anxiety on brain activation to the threat versus safe conditions were tested using stepwise regression. Stepwise regressions were performed by entering anxiety during the brain scan at Step 1, change in cardiac contractility at Step 2, and the interaction between brain scan anxiety and change in cardiac contractility at Step 3 for each region associated with increases in cardiac contractility (see Table 2). For all three areas, contractility predicted a significant proportion of variance in brain activation even after variance predicted by anxiety was removed. Furthermore, a significant proportion of the variance in the right middle frontal and right insula clusters was accounted for by the interaction between self-reported anxiety and cardiac contractility. Conversely, self-reported anxiety and cardiac contractility accounted for unique and independent variance in the left amygdala cluster.

DISCUSSION

The findings from this study highlight the utility of scanning brain and body to study relations between neural and cardiac function in emotion. Moreover, they underscore the importance of individual differences in the neural response to affectively salient stimuli (Davidson, 2000). Threat of shock was associated with increased activation in extensive regions of the right PFC: orbitofrontal, inferior frontal, superior frontal, and middle frontal gyri. It is of interest that for activation in the inferior frontal, superior frontal, and middle frontal gyri there were significantly greater right- than left-sided MR signal changes. Although there was no significant difference between activation in the right versus left orbitofrontal gyrus, only activation in the right orbitofrontal gyrus was significantly greater for the threat versus safe condition. These findings are consistent with a large body of electrophysiological data that has found consistently greater changes in right prefrontal brain electrical measures in response to aversive compared with neutral emotional stimuli (Coan & Allen, 2003; Davidson, 2000).

Significantly greater activation to the threat versus safe conditions was also seen in the bilateral insula cortex. These findings are in line with evidence showing that the insula cortex is implicated in autonomic arousal, awareness, and control (Critchley, Corfield, et al., 2000; Oppenheimer, Kedem, & Martin, 1996; Oppenheimer, 1993), pain perception (Zhang, Dougherty, & Oppenheimer, 1999), and fear responses (Phelps et al., 2001).

Self-reported anxiety in anticipation of a threat of shock was associated with activation in the bilateral

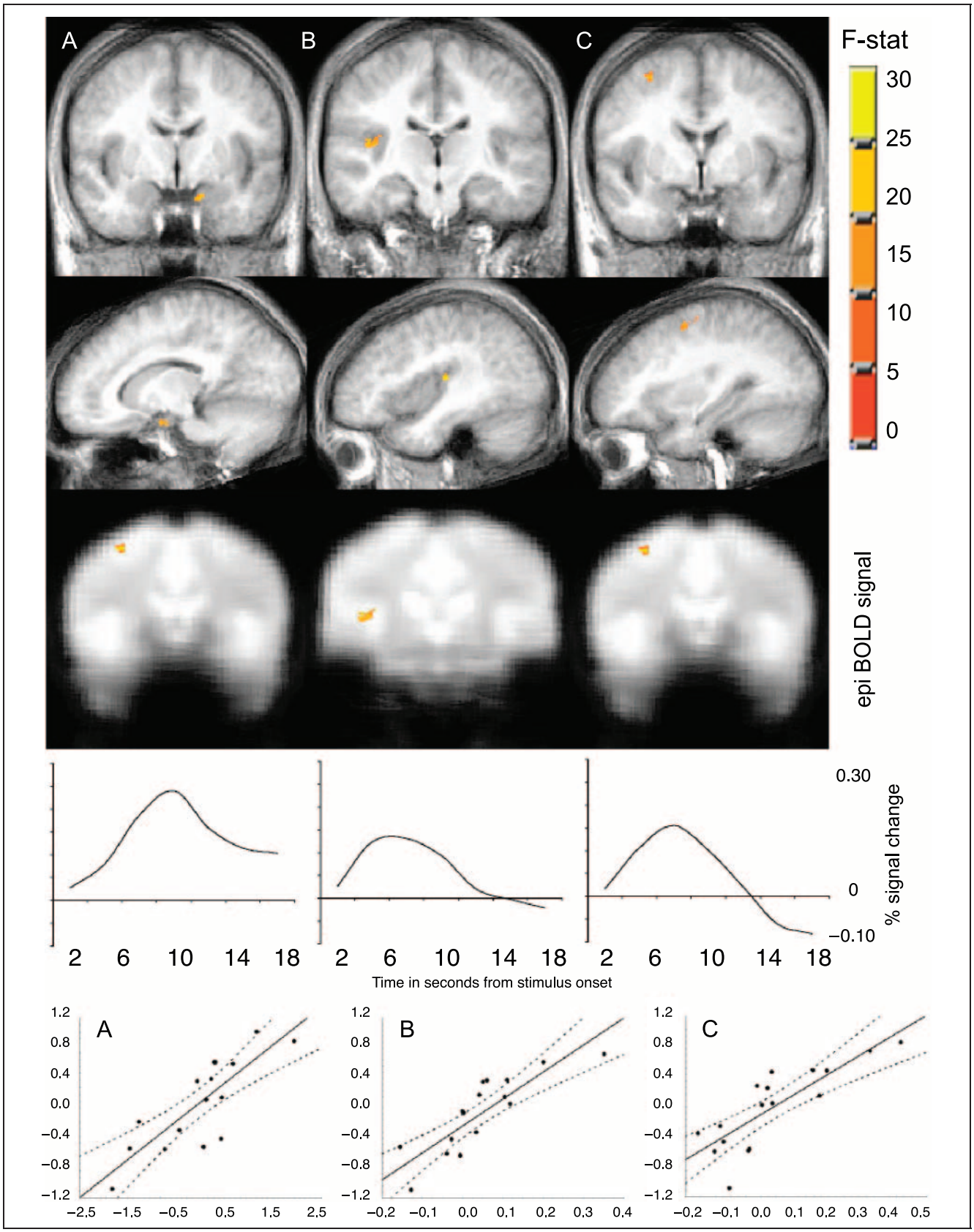
A
B
C
F-stat
30
25
20
15
10
5
0
epi BOLD signal
0.30
0
−0.10
% signal change
2 6 10 14 18
Time in seconds from stimulus onset
A
B
C
1.2
0.8
0.4
0.0
−0.4
−0.8
−1.2
−2.5 −1.5 −0.5 0.5 1.5 2.5
−0.2 −0.1 0.0 0.1 0.2 0.3 0.4
−0.2 −0.1 0.0 0.1 0.2 0.3 0.4 0.5

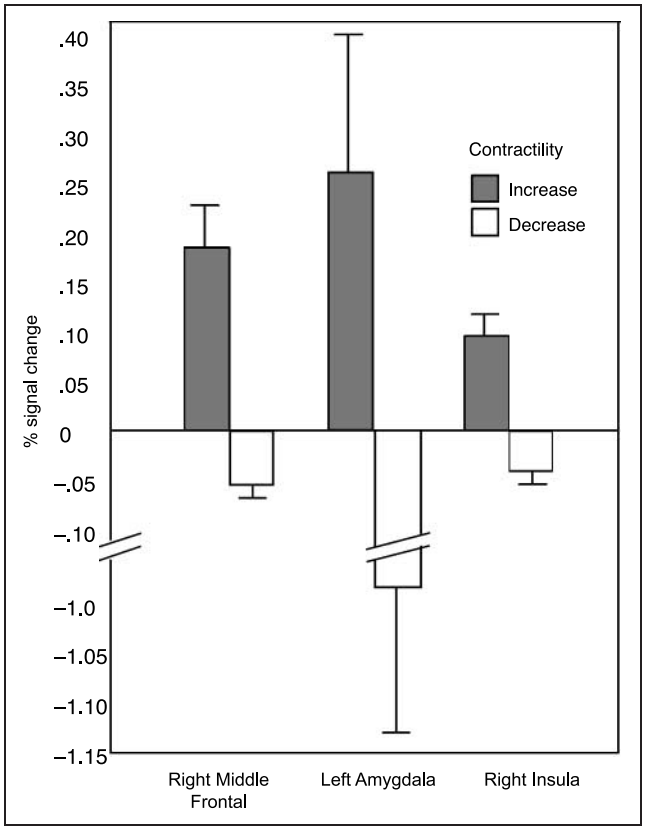

Figure 6. Percent signal change in the left amygdala, right insula, and right middle frontal clusters displayed in Figure 5 broken down by type of cardiac contractility response to the threat versus safety conditions: increase in contractility (n = 10) versus decrease in contractility (n = 7).

Table 2. Regressions Predicting Brain Activation to the Threat versus Safe Conditions Entering Self-reported Anxiety, Cardiac Contractility, and the Interaction between Anxiety and Contractility in a Stepwise Fashion

Step	*r*	*Change R^2*	*F*	*df*	*p*
Left amygdala					
1 Anxiety	.670	.449	11.42	14	.004
2 Contractility	.851	.275	12.94	13	.003
3 Anxiety × Contractility	.855	.007	0.32	12	.57
Right middle frontal					
1 Anxiety	.442	.196	3.65	15	.075
2 Contractility	.822	.480	20.69	14	.0001
3 Anxiety × Contractility	.928	.185	17.31	13	.001
Right insula					
1 Anxiety	.533	.284	5.95	15	.028
2 Contractility	.841	.423	20.19	14	.001
3 Anxiety × Contractility	.928	.155	14.53	13	.002

OFC, right middle frontal gyrus, right insula, left amygdala, and right postcentral gyrus. These regions largely overlap with regions associated with greater activation to the threat versus safe condition, which suggests that conscious awareness of arousal to a potential threat of shock is a component in the circuitry activated to the threat versus safe conditions.

Variations in cardiac contractility were strongly predicted by variations in MR signal change in the right middle frontal gyrus, left amygdala, and right posterior insula. This pattern of association was found although there were no overall differences in cardiac contractility in response to threat versus safety cues. Only 10 of the 17 subjects tested in this experiment showed greater cardiac contractility during the threat compared with safety trials. These were the subjects for whom the threat cues produced more activation than safety cues in affective circuitry of the brain; moreover, subjects who exhibited greater cardiac contractility in response to the threat versus safety cues also reported more subjective anxiety.

Interestingly, cardiac contractility accounted for a significant proportion of the variance in each of these brain regions even after variance accounted for by self-reported anxiety was removed. In addition, the interaction of cardiac contractility and self-reported anxiety accounted for a significant proportion of variance in the right insula and right middle frontal regions even after variance accounted for by self-reported anxiety and cardiac contractility alone were removed. These findings are in line with the idea that these regions may be associated with conscious awareness of aversive stimuli as well as conveying somatosensory states (Critchley, Mathias, et al., 2002; Phelps, et al., 2001; Shi, & Cassell, 1998). Moreover, the conscious awareness of arousal and autonomic state interact and augment the cortical activation in these regions in response to the aversive stimuli. Conversely, both self-reported anxiety and cardiac contractility accounted for a significant proportion

Figure 5. Clusters of brain activation (threat minus safe) positively associated with cardiac contractility to the threat of shock. The first two rows display the location and size of the clusters with the color of the cluster indexing the size of the effect. The third row is composed of the same clusters superimposed on an averaged EPI BOLD signal indicating adequate signal coverage for each cluster. The fourth row is the averaged hemodynamic response function to the threat condition for each cluster. The last row contains the scatter plots for each cluster with the difference in cardiac contractility (threat minus safety) on the x axis and the difference in percent signal change (threat minus safety) for each cluster on the y axis. (A) Left medial amygdala (x = 13, y = −4, z = −18; no. of voxels = 56, r = .82, p < .0001). (B) Right posterior insula (region Id) (x = −36, y = −18, z = 13; no. of voxels = 99, r = .84, p < .0001). (C) Right middle frontal gyrus (posterior region), (x = −29, y = −19, z = 46; no. of voxels = 147, r = .82, p < .0001).

of the variance in the left amygdala, but these effects were independent of one another, suggesting that the cognitive representation of fear is independent of the somatosensory representation in the left amygdala. This finding is in line with those of Phelps et al. (2001) suggesting that the cognitive representation of fear is dependent on the left amygdala.

In summary, these findings support the hypothesis that the left amygdala, extensive regions of the right PFC, and the right insular cortex are involved in stress-related sympathetic cardiac reactivity and suggest a mechanism by which acute negative emotional states may be associated with adverse cardiac responses. When this circuitry is activated over long periods, it may lead to deleterious downstream consequences for the cardiovascular system as a function of excessive sympathetic discharge to the heart, potentially contributing to coronary heart disease. Behavioral and pharmacological treatments that target the emotional circuitry of the brain identified in this report may be efficacious in the downregulation of central mechanisms of sympathetic cardiac control.

METHODS

Participants

Twenty-three right-handed male college students participated in the study. Participants' ages ranged from 18 to 23 years (M = 20, SD = 1.35). They had an average height and weight of 181.35 cm (SD = 5.11) and 77.11 kg (SD = 8.14), respectively. Analyses were restricted to the 17 participants who showed a clear and significant bradycardia to the threat versus safe conditions in order to increase homogeneity of brain–cardiac interactions across participants. All participants reported to be in good cardiovascular health with no known parental or sibling cardiovascular disease. Participants were asked to refrain from caffeine, alcohol, or any over-the-counter medication on the day of the scans. All participants gave informed consent before the administration of any experimental procedures.

Overview

Participants underwent two consecutive MRI scans: one brain MRI and one cardiac MRI. Before both scans the participants filled out both the general and now versions of the State Train Anxiety Inventory (STAI) indexing trait anxiety and state anxiety (anxiety in response to the experimental session itself), respectively. Anxiety ''in anticipation of a shock'' and a rating of pain associated with the shocks were taken directly after each scan. Participants were asked to rate how anxious they were in anticipation of the shocks on a 0 (*not at all anxious*) to 20 (*extremely anxious*) scale and how painful the experienced shocks were on a scale from 0 (*not painful at all*) to 20 (*extremely painful*). None of the participants had any experience with the shocks before the first scan. The task was described to participants and they were told exactly how long each trial and total task length would be before the scans. For the cardiac scan they were also given instructions to hold their breath for a cued amount of time during each trial to minimize thorax movement. No such breath-hold instructions were given for the brain scan.

Threat-of-Shock Task

Participants were asked to lie in an MRI scanner while passively viewing images of four unique geometric objects: red square, blue star, green hexagon, and yellow circle. All of the subjects were told that two of the objects were associated with a 20% chance of a mild electric shock (threat trials), whereas the other two objects were not associated with shock (safety trials). Half of the subjects were told that the red square and blue star were the threat trials, and the green hexagon and yellow circle were safety trials. The associated shock contingencies were reversed for the other half of the subjects. The same shock contingencies were used for both the brain and the cardiac scan within subjects. All subjects underwent a brain and a cardiac MRI scan back-to-back with approximately 10 min in between scans for breakdown and setup. The order of the brain and cardiac scans was counterbalanced across subjects. Sixty trials were presented during the brain scan (30 threat, 30 safety) and 30 trials were presented during the cardiac scan (15 threat, 15 safety). Threat and safety trials were presented in an identical pseudorandom order across subjects. For each trial the geometric object was presented for 3 sec followed by 19 sec of blank screen. Subjects were told that if they saw either of the two threat objects they might receive a shock at any point during the 19 sec of blank screen. Before the first scan two Ag–AgCl shock electrodes were attached to the ankle. The electrodes were connected to shielded leads that were tightly twisted to minimize electromagnetic interference. Shocks (4 mA) were delivered via an isolated physiological stimulator (Coulbourn Instruments, L.L.C., Allentown, PA) with a 20-msec duration. All subjects received three shocks during the brain scan and two shocks during the cardiac scan. All subjects also had an MRI-compatible pulse oximeter cuff attached to their right middle finger during both the brain and cardiac scans. At the end of each scan, subjects were asked how many shocks they actually received. All but one subject verified receiving three shocks during the brain scan and two shocks during the cardiac scan. One subject reported no shocks during the brain scan (most likely due to mechanical failure) and two during the cardiac scan; however, his brain data were not excluded because the ''threat'' of the shock was still present. After

both scans the subjects were asked to rate how anxious they were in anticipation of the shocks and to rate the pain of the shocks received. Afterward, all subjects were debriefed and given monetary compensation for participation.

Pulse Rate Acquisition and Analysis

Pulse rate was processed and visually edited for motion artifact off-line using manufacturer-recommended software, N-vision, along with software derived in-house to calculate average pulse rate at-4 sec intervals across the threat and safe trials within each subject. Pulse rate was averaged across 4-sec chunks across the 19-sec interval immediately following stimulus offset yielding an average pulse rate at 4, 8, 12, and 16 sec poststimulus offset. The change in HR time course across these four points was then plotted for each participant and an average change in HR was calculated across the four time points for each participant. Participants who had an average deceleration of at least 1 bpm to the threat versus safe trials and displayed a consistent bradycardia that reflected an inverse quadratic trend to the threat versus safe trials (i.e., an initial decrease in HR followed by a gradual return to baseline) were classified as ''decelerators'' (see Figure 1). No data had to be eliminated due to motion artifact or equipment malfunction.

Brain fMRI Acquisition and Analysis

Both the brain and cardiac MRI scans were acquired with a GE Signa Horizon 1.5-T scanner equipped with high-speed, whole-body gradients and a whole-head transmit–receive quadrature birdcage head coil (GE Medical Systems, Waukesha, WI). Structural brain images were acquired for anatomical localization of functional activity. For this purpose, a 3-D SPGR volume was acquired (TE = 8 msec, TR = 35 msec, FOV = 24 × 24 cm, flip angle = 30°, NEX = 1, 256 × 256 matrix, 124 axial slices, slice thickness = 1.1–1.2 mm). After the anatomical images were collected, functional data were collected, using whole-brain echo-planar imaging (EPI). Coronal acquisition was used to acquire 23 slices per functional image, with a thickness of 7 mm and a gap of 1 mm. The field of view for each slice was 240 × 240 mm, with a 64 × 64 matrix. The resulting voxel size was 3.75 × 3.75 by 8 mm. A TR of 3 sec was used (TE = 30 msec), and 409 functional images were acquired. Images of the geometric objects were presented in three different timing conditions, such that some images were presented synchronously with the TR and others were asynchronous with the TR (i.e., jittered). These different timing conditions provided an effective time resolution of 1 sec.

Differential brain activation maps were generated by comparing activation to the threat versus safe conditions in a voxelwise manner using analysis of functional neural images (AFNI) version 2.31 software (Cox, 1996). Data processing steps included image reconstruction in conjunction with smoothing in Fourier space via a Hanning window (full width at half maximum = 1 voxel), six-parameter rigid-body motion correction, removal of skull and ghost artifacts, and application of a high-pass temporal Fourier filter that removed frequencies slower than 0.016 Hz. The time series was modeled with a least squares general linear model (GLM) fit to an ideal hemodynamic response function (gamma variate), and the resultant beta weights were converted to percentage signal change. During the GLM fit, the time to onset of response was allowed to vary independently for each voxel from 0 to 4 sec; the same lag was used for both the threat and safe conditions. This variable onset allows for sensitivity to the varying blood perfusion rates across the brain, whereas fixing the time lag as the same for both conditions ensures that the responses are properly separated and estimated. The resultant percentage signal change maps from the GLM were transformed into the standardized Talairach space via identification of anatomical landmarks on the high-resolution SPGR (Talairach & Tournoux, 1988).

To identify differences in brain activation patterns associated with the threat versus safe conditions, whole-brain paired t tests were performed (threat minus safe). An individual p value threshold of $p = .001$ and a minimum cluster size of 50 contiguous voxels was used to control for multiple comparisons. In order to test laterality in regions that were significant in either the right or left hemisphere, significant clusters of interest were dilated out 20% and used to identify the homologous cluster in the opposite hemisphere. Average percentage signal change values from the dilated cluster on the same and homologous side were extracted. All participants had adequate signal in the contralateral hemisphere for each region tested.

Cardiac MRI Acquisition and Analysis

Before the cardiac MRI scan the left side of the subject's chest was shaved and wiped with an abrasive electrode prep (NuPrep). A four-lead, MRI-compatible ECG patch with fiber-optic cables (GE Medical systems, Milwaukee, WI) was then placed under the left nipple at the level of the heart for cardiac MRI gating purposes only; the ECG was not actually recorded. The quality of the ECG was visually verified before proceeding. A strain gauge bellows was then placed around the subject's abdomen to verify compliance of the breath-hold and determine initiation of cardiac MRI acquisition within each trial. All cardiac images were obtained during breath-hold to minimize the effect of thoracic movement on image quality. Subjects were instructed in the proper breath-hold technique before image acquisition. Subjects were told to breath naturally in between trials and to take a breath in when they saw an image of one of the geomet-

ric shapes and then breath it out and hold their breath at full exhalation for approximately 8–10 sec after stimulus offset. Subjects were told that we were monitoring their breathing and that as soon as we saw they were holding their breath on full exhalation we would start acquiring cardiac images. Furthermore, they were told that they would know when cardiac images were being acquired due to the characteristic noises the scanner makes during image acquisition. Subjects were told to continue to hold their breath during image acquisition and that as soon as they heard the scanner stop acquiring images they could resume normal breathing until the next trial. Subjects were instructed to repeat this breath-hold pattern throughout the 30 cardiac trials.

Longitudinal scout images of the heart were obtained and used to select a cross-sectional plane across the maximum width of the left ventricle. Cross-sectional images of the left ventricle were obtained during the breath-hold of each of the 15 safe and 15 threat trials. Images were obtained with a TR = 7 msec and flip angle = 20°. Images were gated based on the R spike from the ECG and were obtained at 28 msec intervals from the initiation of the *R* spike to the end of the T wave across multiple cardiac cycles. Therefore, the number of images and length of breath-hold (i.e., number of required cardiac cycles) varied based on the subject's heart rate, with slower heart rates requiring more images and longer breath-holds to cover the entire cardiac cycle. Length of breath-holds varied between 8 and 12 sec with most being around 10 sec.

Cross-sectional cardiac images were processed and analyzed using in-house software SPAM (Spamalize, Oakes, University of Wisconsin, Madison, WI, tezpur.keck.waisman.wisc.edu/~oakes/spam/spam_frames.htm). Images were first cropped to focus on the left ventricle. Region-of-interest (ROI) analyses were then drawn around the area of the left ventricle in the images corresponding to maximum systole (maximum contraction) and maximum diastole (maximum relaxation). The ROIs were defined in a semiautomated manner as follows: A connected-pixel search was performed starting at a seed point in the wall of the myocardium. A binary mask was constructed composed of pixels that were (1) spatially connected to one another and (2) had a value between a predefined lower and upper threshold. The mask was subsequently edited manually to exclude noncardiac tissue. Cardiac contractility was defined as the difference in area (mm^2) of the left ventricle from maximum diastole to maximum systole.

Correlations were performed between changes in brain activation and cardiac contractility during the threat versus the safe condition. Significant clusters of activation were then extracted using an a priori α value of .05 for the insular cortex and amygdalae. Additional cluster analyses were performed for cortical areas with an α value of .01 to tease apart larger, connected, cortical clusters.

Acknowledgments

We thank Michael Anderle, Katie Horras, Terry Oakes, Hillary Schaefer, Wil Irwin, and Kelli Hellinbrand for technical support. This research was supported from grants from the Charles M. Dana Foundation and National Institute of Mental Health.

Reprint requests should be sent to Kim M. Dalton or Richard J. Davidson, W. M. Keck Laboratory for Functional Brain Imaging and Behavior at the Waisman Center, University of Wisconsin, 1500 Highland Avenue, Madison, WI 53705, or via e-mail: kmdalton@facstaff.wisc.edu or rjdavids@wisc.edu.

The data reported in this experiment have been deposited in the fMRI Data Center (www.fmridc.org). The accession number is 2-2004-1186E.

Note

1. The amygdala cluster lies on the medial edge of the imageable region and hence could reflect movement artifacts related to the abrupt change in signal to noise ratios in this area. However, this explanation is unlikely given the motion correction procedures used and that the cluster lies within the area adequately covered by the EPI and that the averaged MRI time series within the cluster reflects a clear hemodynamic response, not artifactual noise.

REFERENCES

Augustine, J. (1996). Circuitry and functional aspects of the insular lobe in primates including humans. *Brain Research Reviews, 22,* 229–244.

Brownley, K. A., Hurwitz, B. E., & Schneiderman, N. (2000). Cardiovascular psychophysiology. In J. T. Cacioppo, L. G. Tassinary, & G. Berntson (Eds.), *Handbook of psychophysiology.* Cambridge: Cambridge University Press, pp. 224–264.

Buchel, C., Morris, J., Dolan, R. J., & Friston, K. J. (1998). Brain systems mediating aversive conditioning: An event-related fMRI study. *Neuron, 20,* 947–957.

Cechetto, D. F. (1994). Identification of a cortical site for stress-induced cardiovascular dysfunction. *Integrative Physiological & Behavioral Science, 29,* 362–373.

Coan, J. A., & Allen, J. J. (2003). The state and trait nature of frontal EEG asymmetry in emotion. In K. Hugdahl & R. J. Davidson (Eds.), *The asymmetrical brain* (pp. 565–615). Cambridge: MIT Press.

Cox, R. W. (1996). AFNI: Software for analysis and visualization of functional magnetic resonance neuroimages. *Computers and Biomedical Research, 29,* 162–173.

Critchley, H. D., Corfield, D. R., Chandler, M. P., Mathias, C. J., & Dolan, R. J. (2000). Cerebral correlates of autonomic cardiovascular arousal: A functional neuroimaging investigation in humans. *Journal of Physiology, 523,* 259–270.

Critchley, H. D., Mathias, C. J., & Dolan, R. J. (2002). Fear conditioning in humans: The influence of awareness and autonomic arousal on functional neuroanatomy. *Neuron, 33,* 653–663.

Davidson, R. J. (2000). Affective style, psychopathology, and resilience: Brain mechanisms and plasticity. *American Psychologist, 55,* 1196–1214.

Davidson, R. J. (2002). Anxiety and affective style: Role of prefrontal cortex and amygdala. *Biological Psychiatry, 51,* 68–80.

Davis, M., & Whalen, P. J. (2001). The amygdala: Vigilance and emotion. *Molecular Psychiatry, 6,* 13–34.
Grippo, A. J., Moffitt, J. A., & Johnson, A. K. (2002). Cardiovascular alterations and autonomic imbalance in an experimental model of depression. *American Journal of Physiology: Regulatory, Integrative, and Comparative Physiology, 282,* R1333–R1341.
LaBar, K. S., Gatenby, J. C., Gore, J. C., LeDoux, J. E., & Phelps, E. A. (1998). Human amygdala activation during conditioned fear acquisition and extinction: A mixed-trial fMRI study. *Neuron, 20,* 937–945.
Morris, J. S., Ohman, A., & Dolan, R. J. (1999). A subcortical pathway to the right amygdala mediating ''unseen'' fear. *Proceedings of the National Academy of Sciences, U.S.A., 96,* 1680–1685.
Oppenheimer, S. (1993). The anatomy and physiology of cortical mechanisms of cardiac control. *Stroke, 24,* 13–15.
Oppenheimer, S. M., Kedem, G., & Martin, W. M. (1996). Left-insular cortex lesions perturb cardiac autonomic tone in humans. *Clinical Autonomic Research, 6,* 131–140.
Phelps, E. A., O'Connor, K. J., Gatenby, J. C., Gore, J. C., Grillon, C., & Davis, M. (2001). Activation in the left amygdala to a cognitive representation of fear. *Nature Neuroscience, 4,* 437–441.
Rauch, S. L., Savage, C. R., Alpert, N. M., Fischman, A. J., & Jenike, M. A. (1997). The functional neuroanatomy of anxiety: A study of three disorders using positron emission tomography and symptom provocation. *Biological Psychiatry, 42,* 446–452.
Shi, C. J., & Cassell, M. D. (1998). Cascade projections from somatosensory cortex to the rat basolateral amygdala via the parietal insular cortex. *Journal of Comparative Neurology, 399,* 469–491.
Shi, C. J., & Davis, M. (1999). Pain pathways involved in fear conditioning measured with fear-potentiated startle: Lesion studies. *Journal of Neuroscience, 19,* 420–430.
Spyer, K. M. (1994). Annual review prize lecture. Central nervous mechanisms contributing to cardiovascular control. *Journal of Physiology, 474,* 1–19.
Talairach, J., & Tournoux, P. (1988). *Co-planar stereotaxic atlas of the human brain: 3-Dimensional proportional system: An approach to cerebral imaging.* New York: Thieme.
Wittling, W., Block, A., Schweiger, E., & Genzel, S. (1998). Hemisphere asymmetry in sympathetic control of the human myocardium. *Brain & Cognition, 38,* 17–35.
Zald, D. H. (2003). The human amygdala and the emotional evaluation of sensory stimuli. *Brain Research Reviews, 41,* 88–123.
Zhang, Z. H., Dougherty, P. M., & Oppenheimer, S. M. (1999). Monkey insular cortex neurons respond to baroreceptive and somatosensory convergent inputs. *Neuroscience, 94,* 351–360.